# Low-threshold two-photon pumped ZnO nanowire lasers

**Chunfeng Zhang,[1] Fan Zhang,[1] Tian Xia,[1] Nitin Kumar,[2] Jong-in Hahm,[2] Jin Liu,[3] Zhong Lin Wang[3], and Jian Xu,[1,*]**

[1] *Department of Engineering Science and Mechanics, The Pennsylvania State University, 212 Earth and Engineering Science Building, University Park, Pennsylvania 16802, USA*

[2] *Department of Chemical Engineering, The Pennsylvania State University, 160 Fenske Laboratory, University Park, Pennsylvania 16802, USA*

[3] *School of Materials Science and Engineering, Georgia Institute of Technology, 771 Ferst Dr. N.W., Atlanta, GA 30332*

[*] *Corresponding author: jianxu@engr.psu.edu*

**Abstract:** We report in this communication the two-photon absorption (TPA)-induced room-temperature lasing performance of ZnO nanowires. Under femtosecond pulse-excitation at $\lambda$ = 700 nm in the infrared regime, a remarkably low threshold of 160μJ/cm$^2$ was observed for the TPA-induced lasing action, which is of the same order of magnitude as that measured for the linear lasing process. Time-resolved photoluminescence characterization of two-photon pumped ZnO nanowires reveals the presence of a fast decay (3-4 ps) in the stimulated emission as compared to the slow decay (50-70 ps) for the spontaneous emission. The TPA process in ZnO nanowires was characterized with the nonlinear transmission measurement, which uncovers an enhanced TPA coefficient, about 14.7 times larger than that of bulk ZnO samples. The observed TPA enhancement in ZnO nanowires accounts for the low threshold lasing behavior, and has been attributed to the intensified optical field confined within the nanowire waveguides.



**OCIS codes:** (190.4180) Multiphoton processes; (140.5960) Semiconductor lasers.

## References and links

1. M. H. Huang, S. Mao, H. Feick, H. Q. Yan, Y. Y. Wu, H. Kind, E. Weber, R. Russo, and P. D. Yang, "Room temperature ultraviolet nanowire nanolasers," Science **292**, 1897-1899 (2001).
2. C. Baratto, E. Comini, G. Faglia, G. Sberveglieri, M. Zha, and A. Zappettini, "Metal Oxide nanocrystals for gas sensing," Sens. Actuators B **109**, 2-6 (2005).
3. D. Sirdhar, J. N. Xie, J. K. Abraham, and V. K. Varadan, "Synthesis and photonic property study of ZnO nanowires for a real time photodynamic therapy monitoring probe," Proc. SPIE **6528**, 6528L (2007).
4. Y. F. Zhang and R. E. Russo, "Quantum efficiency of ZnO nanowire nanolasers," Appl. Phys. Lett. **87**, 043106-043108 (2005).
5. D. M. Bagnall, Y. F. Chen, Z. Zhu, T. Yao, M. Y. Shen, and T. Goto, "High temperature excitonic stimulated emission from ZnO epitaxial layers," Appl. Phys. Lett. **73**, 1038-1040 (1998)
6. H. J. Zhou, M. Wissinger, J. Fallert, R. Hauschild, R. Stelzl, C. Klingshirn, and H. Kalt, "Ordered, uniform-sized ZnO nanolaser arrays," Appl. Phys. Lett. **91**, 181112-181114 (2007).
7. C. F. Zhang, Z. W. Dong, G. J. You, S. X. Qian, and H. Deng, "Multiphoton route to ZnO nanowire lasers," Opt. Lett. **31**, 3345-3347 (2006).
8. C. F. Zhang, Z. W. Dong, G. J. You, R. Y. Zhu, S. X. Qian, H. Deng, H. Cheng, and J. C. Wang, "Femtosecond pulse excited two-photon photoluminescence and second harmonic generation in ZnO nanowires," Appl. Phys. Lett. **89**, 042117-042119 (2006).
9. E. V. Chelnokov, N. Bityurin, I. Ozerov, and W. Marine, "Two-photon pumped random laser in nanocrystalline ZnO," Appl. Phys. Lett. **89**, 171119-171121 (2006).
10. E. L. Portnoi, G. B. Venus, A. A. Khazan, I. M. Gadjiev, A. Y. Shmarcev, J. Frahm, and D. Kuhl, "Superhigh-power picosecond optical pulses from Q-switched diode laser," IEEE J. Sel. Top. Quant. Electron. **3**, 256-260 (1997).
11. S. Vainshtein, J. Kostamovaara, M. Sverdlov, L. Shestak, and V. Tretyakov, "Laser diode structure for the generation of high-power picosecond optical pulses," Appl. Phys. Lett. **80**, 4483-4485 (2002).

#107588 - $15.00 USD Received 3 Mar 2009; revised 22 Apr 2009; accepted 22 Apr 2009; published 28 Apr 2009

12. N. Kumar, A. Dorfman, and J. Hahm, "Fabrication of optically enhanced ZnO nanorods and microrods using novel biocatalysts," J. Nanosci. Nanotech. **5**, 1-4 (2005).
13. C. Rullière, *Femtosecond Laser Pulses—Principles and Experiments* (Springer-Verlag, Berlin, 1998).
14. G. P. Banfi, V. Degiorgio, D. Fortusini, and M. Bellini, "Measurement of the two-photon absorption coefficient of semiconductor nanocrystals by using tunable femtosecond pulses," Opt. Lett. **21**, 1490-1492 (1996).
15. J. C. Johnson, K. P. Knutsen, H. Q. Yan, M. Law, Y. F. Zhang, P. D. Yang, and R. J. Saykally, "Ultrafast carrier dynamics in single ZnO nanowire and nanoribbon lasers," Nano. Lett. **4**, 197-204 (2004).
16. W. M. Kwok, A. B. Djurisic, Y. H. Leung, W. K. Chan, D. L. Philips, H. Y. Chen, C. L. Wu, S. Gwo, and M. H. Xie, "Study of excitonic emission in highly faceted ZnO rods," Chem. Phys. Lett. **412**, 141-144 (2005).
17. J. Bolger, A. K. Kar, B. S. Wherrett, R. DeSalvo, and D. J. Hagan, "Nondegenerate two-photon absorption spectra of ZnSe, ZnS, and ZnO," Opt. Commun. **97**, 203-209 (1993).
18. Z. W. Dong, C. F. Zhang, G. J. You, X. Q. Qiu, K. J. Liu, Y. L. Yan, and S. X. Qian, "Multi-photon excitation UV emission by femtosecond pulses and nonlinearity in ZnO single crystal," J. Phys. Condens. Matter **19**, 216202-216208 (2007).
19. X. J. Zhang, W. Ji, and S. H. Tang, "Determinatin of optical nonlinearities and carrier lifetime in ZnO," J. Opt. Soc. Am. B **14**, 1951-1955 (1997).
20. J. He, Y. L. Qu, H. P. Li, J. Mi, and W. Ji, "Three-photon absorption in ZnO and ZnS crystals," Opt. Express **13**, 9235-9247 (2005).
21. X. H. Yang, J. M. Hays, W. Shan, and J. J. Song, "Two-photon pumped blue lasing in bulk ZnSe and ZnSSe," Appl. Phys. Lett. **62**, 1071-1073 (1993).
22. W. Wuenstel and C. Klingshirn, "Tunable laser-emission from wurtzite-type II-VI compounds," Opt. Commun. **32**, 269-273 (1980).
23. L. W. Tutt and T. F. Boggess, "A review of optical limiting mechanisms and devices using organics, fullerenes, semiconductors and other materials," Prog. Quantum Electron. **17**, 299-338 (1993).
24. J.C. Knight, "Photonic crystal fibers," Nature **424**, 847-851 (2003).
25. G. A. Siviloglou, S. Suntsov, R. El-Ganainy, R. Iwanow, G. I. Stegeman, and D. N. Christodoulides, "Enhanced third-order nonlinear effects in optical AlGaAs nanowires," Opt. Express, **14**, 9377-9384 (2006).
26. A. V. Maslova, M. I. Bakunov, and C. Z. Ning, "Distribution of optical emission between guided modes and free space in a semiconductor nanowire," J. Appl. Phys. **99**, 024314-024323 (2006).
27. H. Yoshikawa and S. Adachi, "Optical constants of ZnO," Jpn. J. Appl. Phys. **36**, 6237-6243 (1997).

## 1. Introduction

Recently, nanoscale ultraviolet (UV) lasers based on ZnO nanowires have attracted much attention for their potential applications in integrated photonics, sensing and photochemotherapy [1-3]. Room-temperature UV lasing from ZnO nanowires exhibits high external differential efficiency up to 60%, which was attributed to the marriage of large exciton binding energy and strong optical confinements in ZnO nanostructures [4]. Dynamic analysis on the stimulated emission of ZnO nanowires indicates that a ZnO nanolaser can potentially have temperature-insensitive optical-gain threshold, narrow emission lines, as well as high-temperature stability [5,6]. As promising as the emerging ZnO nanolasers are, ZnO nanowires require optical excitation or pumping with deep-UV, coherent light to produce stimulated emission via a linear optical process. The excitation photon energy has to be larger than the band gap (~3.37 eV) of ZnO nanowires in order to pump them in the one-photon absorption (OPA) regime. The dependence on expensive, deep-UV pumping sources could significantly hinder the applications of ZnO nanolasers in view of the overall cost, complexity, and incompatibility for chip-level integration.

Multi-photon absorption-induced emission process in ZnO nanowires provides an alternative approach to circumvent this limitation. Upon near-infrared (IR) radiation with nanosecond or femtosecond pulses, the nonlinear interaction between the applied optical field and ZnO nanostructures leads to the simultaneous absorption of two or more photons of sub-bandgap energy through a virtual-state assisted interband transition, producing electron-hole pairs in the excited states and, subsequently, the band-edge emission via their radiative recombination [7-9]. Near-IR light pulses are readily produced with inexpensive, (In,Al,Ga)(As,P) laser diodes [10,11], allowing for the chip-level design and low-cost implementation of ZnO nanolasers in photonic circuitries and sensing systems.

#107588 - $15.00 USD Received 3 Mar 2009; revised 22 Apr 2009; accepted 22 Apr 2009; published 28 Apr 2009

Recently, stimulated emission and UV lasing actions via near-IR excitation have been demonstrated in ZnO nanowires, for the first time, by Zhang et al [7]. A sharp lasing peak with ≤ 0.5 nm linewidth was observed from ZnO nanowires pumped by femtosecond pulses at the wavelength near 800 nm. The emission process has been attributed to the band-edge transition induced by the off-resonant two-photon absorption (TPA) in the wide band gap nanostructures. However, a high excitation threshold of 80mJ/cm$^2$ was reported, resulting in a substantially low efficiency for producing up-converted emission in ZnO nanowires.

We report in this letter the resonant TPA-induced lasing performance in ZnO nanowires. Room temperature laser operation at a remarkably low threshold of ~160μJ/cm$^2$ was demonstrated with femtosecond pulse-excitation at 700 nm. Distinct cavity modes were resolved from the laser emission spectra. Time-resolved photoluminescence (TRPL) characterization of two-photon pumped ZnO nanowires reveals the presence of a fast decay (3-4 ps) in the stimulated emission as compared to the slow decay (50-70 ps) for the spontaneous emission. The TPA process in ZnO nanowires arrays was characterized with the nonlinear transmission technique, which shows an enhanced TPA coefficient, about 14.7 times larger than that of bulk ZnO samples. The observed TPA enhancement in ZnO nanowires accounts for the low threshold lasing behavior, and can be attributed to the intensified optical field confined within the nanowire waveguides.

## 2. Experimental methods

The ZnO nanowire samples used in the study were fabricated using a straightforward method with biocatalysts, which has been reported elsewhere [12]. The synthesized nanowires samples were characterized by scanning electron microscopy (SEM). The SEM images of the synthesized nanowires in Fig. 1 illustrate the size and shape of the as prepared ZnO nanowires. The average diameter and length of the ZnO nanowires are ~180 nm and ~10 μm, respectively. XRD characterization of ZnO nanowires indicates that these ZnO materials exhibit wurtzite structures and that the c-axis is the preferential growth direction. The end and side facets of an individual ZnO nanowire are clearly illustrated in the SEM panels (Fig 1(b) and (c)), revealing the well-defined, single-crystalline nanowire structure without noticeable defects.

For the PL and lasing characterization of ZnO nanowires, the pumping beam was focused on the sample with an incident angle of 45° with respect to the symmetric axis of nanowires, and the emission from ZnO nanowires was collected along the symmetric axis. Time integrated emission spectra were recorded by a spectrometer equipped with photomultiplier tubes (SpectroPro 500i, ~ 0.05 nm spectral resolution). The excitation pulses were produced by an optical parameter amplifier (TOPAS, Coherent) pumped with the amplification stage of a Ti:Sapphire laser (Libra, 1 kHz, 80 fs, Coherent Inc.) with the tunable output wavelength ($\lambda_{exc}$) near 700 nm. TRPL characterization of two-photon pumped ZnO nanowires was performed with the Kerr shutter technique [13]. A $CS_2$ liquid cell was used as the Kerr medium with the temporal resolution of ~1 ps. The fluence energy of the probe pulse was varied below and above the lasing threshold of the two-photon pumped ZnO nanowires for comparison. For the nonlinear-absorption characterization of ZnO nanowires, the intensity of the femtosecond laser beam was altered continuously by a variable attenuator consisting of two crossed Glan polarizers and a Babinet compensator used as tunable zero-order λ/2 plate [14]. All of the experiments were carried out at room temperature.

## 3. Results and discussions

Figure 2(a) shows the emission spectra of two-photon pumped ZnO nanowires for the excitation fluence of 100 μJ/cm$^2$, 160 μJ/cm$^2$, and 215 μJ/cm$^2$, respectively. At a relatively low excitation energy (100 μJ/cm$^2$), the PL signal exhibits a wide bandwidth centered at ~ 388 nm with a full width at half maximum (FWHM) of ~ 20 nm, representing the TPA-induced spontaneous emission. When the excitation fluence reaches 160 μJ/cm$^2$, the emission displays an abrupt narrowing of the FWHM bandwidth down to ≤1 nm, suggesting the transition from

#107588 - $15.00 USD Received 3 Mar 2009; revised 22 Apr 2009; accepted 22 Apr 2009; published 28 Apr 2009

TPA-induced spontaneous emission to TPA-induced lasing action in ZnO nanowires [6]. Upon further increasing the excitation fluence, the enhanced gain in ZnO nanowires allows for the stimulated emission of multiple longitudinal modes. Distinct cavity modes were resolved from the laser emission spectra. The dominant mode, peaked at 390nm, exhibits a narrow linewidth of ~ 0.2 nm. The inset of Fig 2(a) is the photomicrograph of a lasing ZnO nanowire pumped at 215 μJ/cm$^2$.

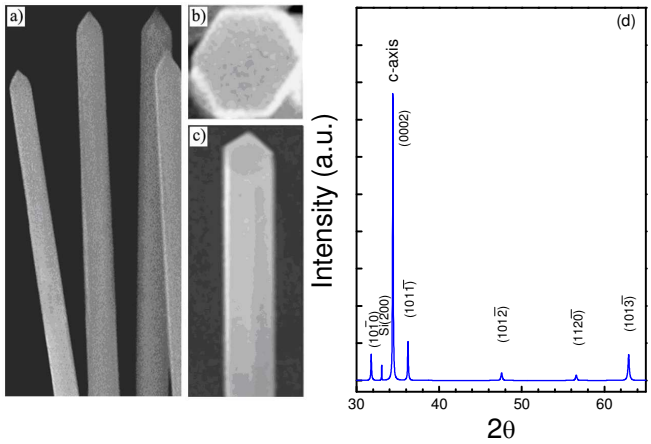


Fig. 1. (a) The 1.2 x 3 μm SEM micrograph displays as-grown structures of the gas-phase synthesized ZnO nanowires used in the lasing experiments. The average diameter and length of ZnO nanowires are 180 nm and 10 μm, respectively. ZnO nanowires, preferentially grown along the c-axis, exhibit wurtzite structures with hexagonal end facets. The end and side facets of an individual ZnO nanowire are clearly shown in the SEM panels (b) (200 x 200 nm) and (c) (420 x 1000 nm), respectively. (d) Typical X-ray diffraction pattern of the synthesized ZnO nanowires.

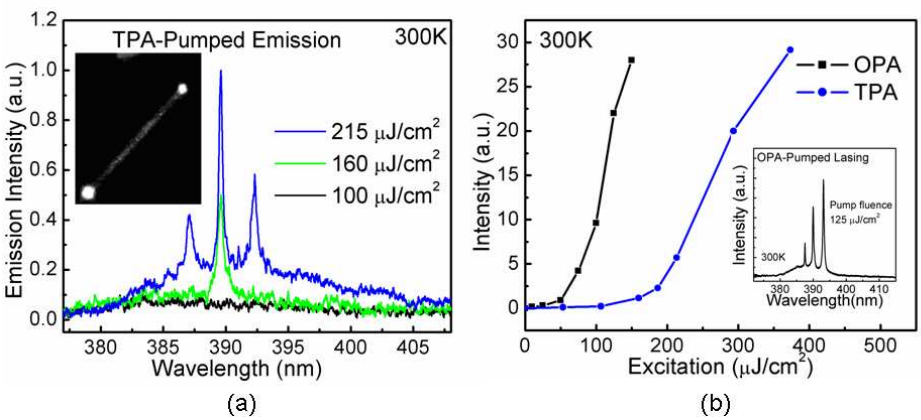


Fig. 2. (a) Two-photon pumped emission spectra from ZnO nanowires for difference excitation fluence. The inset of (a) is the photomicrograph of a lasing ZnO nanowire pumped in the TPA regime. (b) Integrated emission intensity from ZnO nanorods pumped by single-photon and two-photon processes versus excitation fluence. The inset of (b) shows the one-photon pumped lasing spectrum of ZnO nanowires.

Figure 2(b) plots the integrated emission intensities as functions of the excitation fluence for ZnO nanowires pumped in OPA ($\lambda_{pump}$= 350 nm) and TPA ($\lambda_{pump}$= 700 nm) regimes, respectively. The threshold behavior of the two-photon pumped lasing action of ZnO nanowires ($\lambda_{pump}$ = 700 nm) is clearly revealed in the plot with a threshold fluence of 160 μJ/cm$^2$. It is worth noting that the observed threshold of TPA-induced lasing is over two

#107588 - $15.00 USD Received 3 Mar 2009; revised 22 Apr 2009; accepted 22 Apr 2009; published 28 Apr 2009

orders of magnitude lower than the early reported values (from ~ 0.67 TW/cm$^2$ to ~ 2 GW/cm$^2$ in term of peak power), and differs from the threshold of OPA-induced lasing (~ 0.63 GW/cm$^2$) only by a factor of three in our experiment. The output spectrum of ZnO nanowire lasing via one photon pumping is presented in the inset of Fig. 2(b), which largely matches the TPA-induced multimode lasing in the same nanowire sample (Fig. 2(a)).

In the present study, the two-photon pumping scheme is implemented with the excitation wavelength of λ=700 nm. The photon energy, $E_{hv}$ (700 nm), is greater than half of the band gap of ZnO nanowires ($E_g$(ZnO)), whereby the energy of two incident photons is sufficient to produce excitons or electron-hole pairs via virtual state-assisted band-edge transition. Such a resonant TPA process is significantly more efficient than the off-resonance TPA process reported earlier, wherein the excitation light of λ=800 nm has the photon energy $E_{hv}$(800nm) < $E_g$(ZnO) /2.[7] The change from the off-resonant to resonant pumping scheme is believed to account for the dramatic reduction of the lasing threshold in two-photon pumped ZnO nanowires observed herein.

The OPA-induced stimulation emission in ZnO nanowires has been reported to arise from the radiative recombination via exciton scattering and/or electron-hole plasma that were characterized with the lifetimes of 4-9 ps and ≤ 5 ps, respectively [15,16]. To investigate the mechanism of TPA-induced stimulation emission in ZnO nanowires, TRPL measurement was performed for different excitation fluence. Figure 3 plots the transient decays of ZnO nanowire-emission following the femtosecond pulse excitation (τ~80 fs, λ~700nm) with the fluence energy varied below and above the threshold (160 μJ/cm$^2$), respectively. A lifetime of ≥ 50 ps was measured for the TPA-induced spontaneous emission in ZnO nanowires under low fluence-excitation condition, representing a typical free-exciton recombination process. In contrast, a very fast decay with lifetime 3-4 ps, comparable to that of the OPA-induced stimulated emission, together with a slower component, appears in the TRPL curve upon high fluence-excitation. It is suggested by analogy with the OPA-induced process that the faster component can be assigned to the TPA-induced stimulated emission originating from a similar, many-particle effect-associated recombination mechanism. The slower component is caused by the spontaneous emission background.

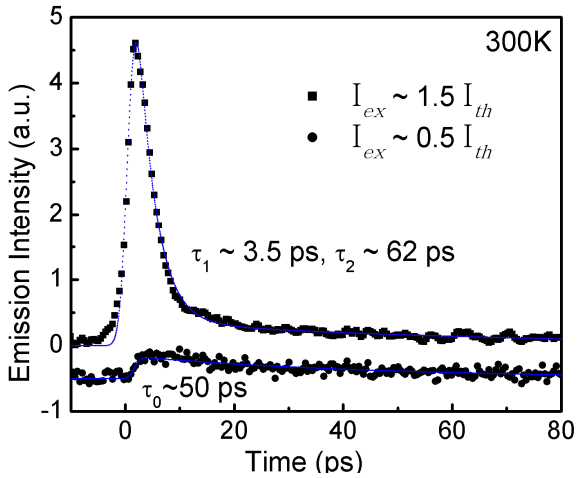


Fig. 3. TRPL traces of two-photon pumped emission from ZnO nanowires with the excitation fluence below and above the lasing threshold.

In bulk semiconductors, TPA is a third order nonlinear optical process characterized with a significantly lower efficiency than that of OPA [17-20]. The thresholds for TPA-induced lasing in bulk ZnSe, ZnSSe, and ZnO, are, consequently, two or three orders of magnitude higher than are achieved in OPA-induced lasing processes [21,22]. However, the present study has revealed a remarkably low threshold for TPA-induced lasing in ZnO nanowires, at the same order of magnitude as was measured for the linear lasing process. In attempts of

#107588 - $15.00 USD Received 3 Mar 2009; revised 22 Apr 2009; accepted 22 Apr 2009; published 28 Apr 2009

explaining the observed low-threshold behavior, the nonlinear transmission of a ZnO nanowire array film, grown on a transparent sapphire substrate, was measured as the function of the incident energy. The average diameter and length of the nanowires in the film are ~180 nm and ~5 μm, respectively, and the average density of the nanowire is ~$6.0\times10^8$ $cm^{-2}$, as illustrated by the SEM image of the nanowire film (inset of Fig. 4). A 0.5mm-thick bulk ZnO crystal was used as the reference sample in the measurement.

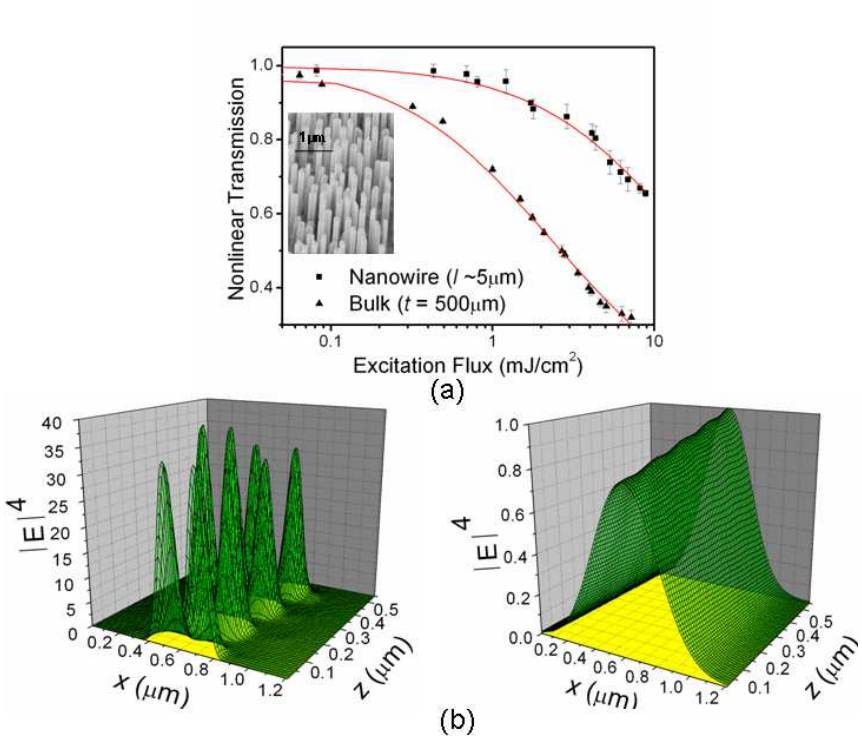


Fig. 4. (a) Nonlinear transmission curves of a ZnO nanowire film and a bulk ZnO crystal, respectively, at λ=700nm, with a peak excitation intensity of ~50 GW/cm$^2$. The inset shows the SEM image of the nanowire film sample. (b) Calculated E-field distribution ($|E|^4$) in sections of nanowire and bulk ZnO samples. (The dashed lines indicate the section boundaries.)

In the nonlinear transmission measurement, the linear scattering loss of the probe light crossing the film of the nanowire array was first determined at a substantially low intensity (~0.01uJ/cm$^2$), allowing for the elimination of the scattering effect in the nonlinear optical characterization. The TPA coefficient of the sample, β, was estimated by the least square fitting to the nonlinear transmission expression derived with a hat-top pulse shape approximation [23]:

$$T_{NL}(I)=\frac{\ln(1+\beta IL)}{\beta IL}, \quad (1)$$

where I is peak intensity of the incident laser beam inside the medium, and L the sample thickness. In the experiment, the beam was focused onto the samples with an f =20 cm lens with 60% of the energy smoothly distributed in a focal spot of 100μm, yielding a peak intensity of 12.5 GW/cm$^2$ for an 80 fs-pulse of 1mJ/cm$^2$. By attenuating the incident light progressively, the nonlinear transmission of both bulk and nanowire ZnO samples at λ= 700 nm were recorded as a function of the impinging energy, the traces of which were plotted in Fig. 4. From the transmission data the TPA coefficient of the bulk ZnO crystal, $\beta_{bulk}$, was determined to be ~ 3.4 cm/GW, in good agreement with the previous studies [19,20]. In contrast, a large 'effective' TPA coefficient of $\beta_{eff}$ = 49.9 cm/GW was obtained for ZnO nanowire arrays by assuming that the peak intensity of the laser beam in the nanowire array is the same as that in the bulk crystal.

#107588 - $15.00 USD Received 3 Mar 2009; revised 22 Apr 2009; accepted 22 Apr 2009; published 28 Apr 2009

The effective TPA coefficient of ZnO nanowires obtained herein represents a ~14.7 fold-enhancement over the intrinsic value for ZnO bulk materials, $\beta_{int}$. The origin of the observed enhancement can be interpreted by examining the quadratic dependence of TPA on the local field intensity of the light:

$$\left(\frac{dI_{NW}(r,z)}{dz}\right)_{TPA} = -\beta_{eff} I_{inc}^{2}(r,z) = -\beta_{int} I_{NW}^{2}(r,z) \quad (2)$$

where $I_{inc}(r,z)$ is the intensity of the incident light at the front surface of the nanowire sample, and $I_{NW}(r,,z)$ the local intensity of the incident light propagating along the symmetric axis (z) of nanowires. If the local intensity of the incident light in ZnO nanowires is greater than that in the bulk crystal, the effective TPA coefficient of ZnO nanowires can be enhanced over the bulk value by a factor of $(I_{NW}/I_{inc})^2$. It has been reported that the optical field in a ZnO nanowire is subject to the tight modal confinement due to the strong index contrast for the nanowaveguide structure [24,25]. In addition, light resonance can take place in a Fabry-Perot cavity formed by such a nanowire waveguide ending with faceted mirrors, which further reinforces the field inside the nanowire [26]. It is, therefore speculated that the intense, localized optical field in the ZnO nanowires leads to the enhanced TPA of the pump light ($\lambda$= 700 nm), which in turn, gives rise to the low-threshold operation of the TPA-induced lasing. In contrast, the efficiency of two-photon pumping in bulk ZnO remains low due to the absence of local field-enhancement.

The speculation was further confirmed by performing the finite-difference time-domain (FDTD) calculation to determine the electric field distribution, $|E(r,z)|^2$, in ZnO nanowires under $\lambda$=700nm light-illumination. In the calculation, the z axis was along the symmetric axis of the nanowire, and the x axis was normal to the symmetric axis in a cross-sectional plane of the wire. Perfectly matched layers were used to absorb any radiation impinging on the domain boundaries that are assigned far from the nanowire surfaces. The field of Gaussian cross sectional-profile was launched from a spatial location outside the nanowire, propagating along z-axis, and incident on the nanowire from the end. The dimensions of the ZnO nanowire used in the calculation were chosen to be the same as those of the nanowires used in the nonlinear transmission measurement, i.e. 180 nm in diameter and 5 μm in length. An inter-nanowire distance of 400 nm was assumed, giving rise to a nanowire density of $6.25\times10^8$ $cm^{-2}$ in the calculation. Light propagation in a bulk ZnO crystal was also modeled in our computation for the sake of comparison.

Figure 4(b) compares the computed field distribution in a linear array of four parallel ZnO nanowires and that in a bulk crystal. The fourth power of the field magnitude i.e., the quartic vale ($|E|^4$), was used in the comparison in view of the fact the effective 2PA coefficient, $\beta_{eff}$, exhibits the quadratic dependence on the local light intensity, $(I_{NW})^2$, of the incident light in ZnO nanowires. In the graph the magnitudes of both fields have been normalized to the peak field in the bulk crystal. Our calculation result indicates that the optical field in a ZnO nanowire is subject to the tight modal confinement, and under resonance condition, the peak magnitude of the quartic electric field ($|E|^4$) in a ZnO nanowire of 180nm-diameter is ~ 40 times higher than that in a bulk ZnO material. When the computed field distribution is spatially averaged for bulk and nanowire samples, respectively, the ratio is reduced to ~12, which agrees well with the measurement result (~14.7). It is therefore concluded that the intensified modal field in ZnO nanowires, in combining with the quartic field dependence of the TPA process, gives rise to the substantially enlarged TPA coefficient, which, in turn, leads to the very low threshold-TPA lasing in ZnO nanowires.

Finally, it is worth mentioning that the observed difference in TPA efficiency between ZnO nanowires and bulk materials is not present for the linear OPA process. The linear absorption coefficient of the crystalline ZnO at $\lambda$=300 nm is as high as $2\times10^5$ $cm^{-1}$ [27], which translates to a short penetration depth of ~50nm for the UV light propagating in ZnO wires. The UV pump light is not subject to any confinement in ZnO nanowaveguides due to the strong absorption. There is essentially no local field enhancement for UV excitation in ZnO nanowires.

#107588 - $15.00 USD Received 3 Mar 2009; revised 22 Apr 2009; accepted 22 Apr 2009; published 28 Apr 2009

**Acknowledgments**

The work is supported by the Army Research Office under Grants DAAD19-02-D-0001. The authors thank Professors Judith A. Todd and Carlo Pantano at Penn State University for the supports on establishing and accessing femtosecond laser facilities in the Center for Multiscale Wave-Materials Interactions.

#107588 - $15.00 USD Received 3 Mar 2009; revised 22 Apr 2009; accepted 22 Apr 2009; published 28 Apr 2009